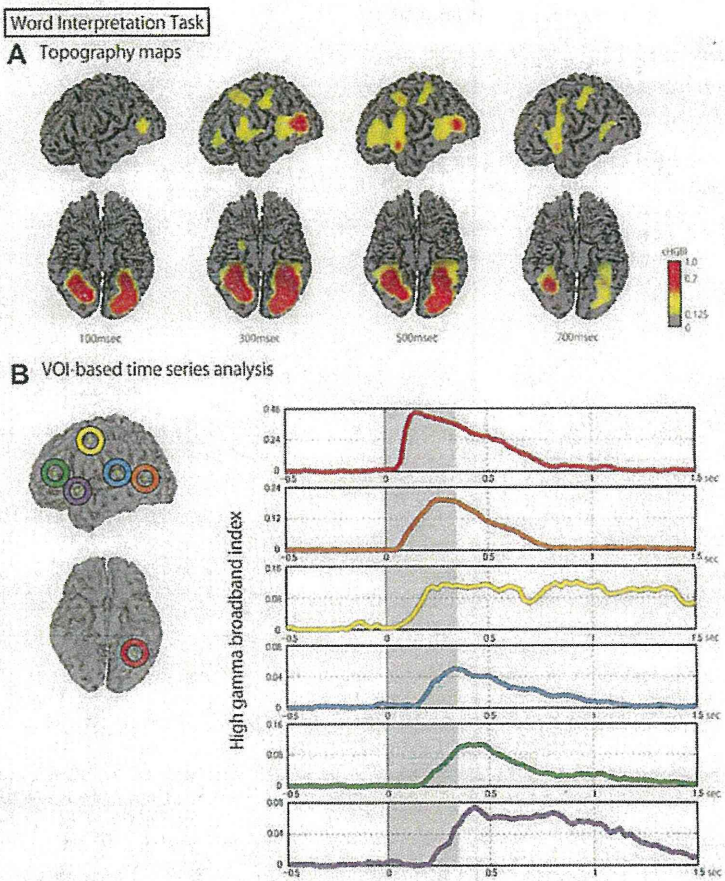

Fig. 3. Word interpretation results. (A) Topographic maps of the high gamma broadband index values (HGBI with electrode density correction) for the word interpretation task. HGBI profiles were aligned on the brain surface at representative time points, indicating sequential activation of the fusiform gyrus (FuG), posterior middle temporal gyrus (pMTG), ventral premotor cortex (vPMC), and middle and inferior frontal gyri (MFG and IFG). (B) HGBI time series of each volume of interest (VOI). The VOI included the FuG (Red), pMTG (Orange), vPMC (Yellow), the superior temporal gyrus (Blue), and the MFG (Green) and IFG (Purple). Each VOI and the corresponding HGBI line are shown in the same color. The gray zones indicate the duration of stimulus presentation. Note the differences in the vertical axis scales among different VOI.

3.3.2. VOI-based time series analysis of HGA during different tasks

To quantitatively evaluate HGA dynamics, we set VOI (radius 15 mm) in the following six cortical areas: FuG, pMTG, STG, vPMC, MFG, and IFG. These areas were chosen because they demonstrated marked HGA augmentation. Figs. 3–5B illustrates the time courses of the averaged raw HGBI within each VOI for each task.

In the WI task, HGA augmentation in the FuG occurred first, beginning at around 100 ms, and the pMTG was recruited slightly later. The FuG augmentation declined after the termination of the visual stimuli, while the vPMC displayed prolonged response between 200 and 1000 ms. Both the MFG and IFG were involved at around 300 ms. The MFG augmentation rapidly decreased at around 400 ms, whereas the IFG augmentation was sustained until 1000 ms (Fig. 3B).

In the PN task, the FuG augmentation occurred first, beginning at around 100 ms and was sustained for more than 1000 ms, reflecting the longer stimulus presentation time of this task. On the other hand, the HGA augmentation of the pMTG occurred slightly later than that observed during the WI; i.e., from 200 ms to 700 ms. The vPMC showed prolonged augmentation between 300 and 900 ms during the PN task, which was similar to that seen during the WI task. The MFG and IFG demonstrated low HGBI values during this task (Fig. 4B).

The initial response related to the VG task involved prominent HGA augmentation of the STG between 100 and 600 ms. The next peaks appeared simultaneously in the pMTG, IFG, and MFG and then gradually decreased until 1000 ms. An interesting characteristic of the HGBI profile for this task was late onset of vPMC response, which appeared at around 500 ms and peaked at around 1000 ms (Fig. 5B).

VOI-based time series analysis demonstrated different HGBI profiles for each task.

4. Discussion

We demonstrated the spatiotemporal dynamics of the brain oscillations related to three different language tasks using a novel method in which we superimposed ECoG-HGA from 21 patients onto a normalized brain. The HGA-dynamics for the WI task demonstrated posterior-to-anterior sequences of cortical recruitment involving the FuG, pMTG, vPMC, MFG, and IFG. Although similar dynamics was observed during the PN task, little HGA was ob-

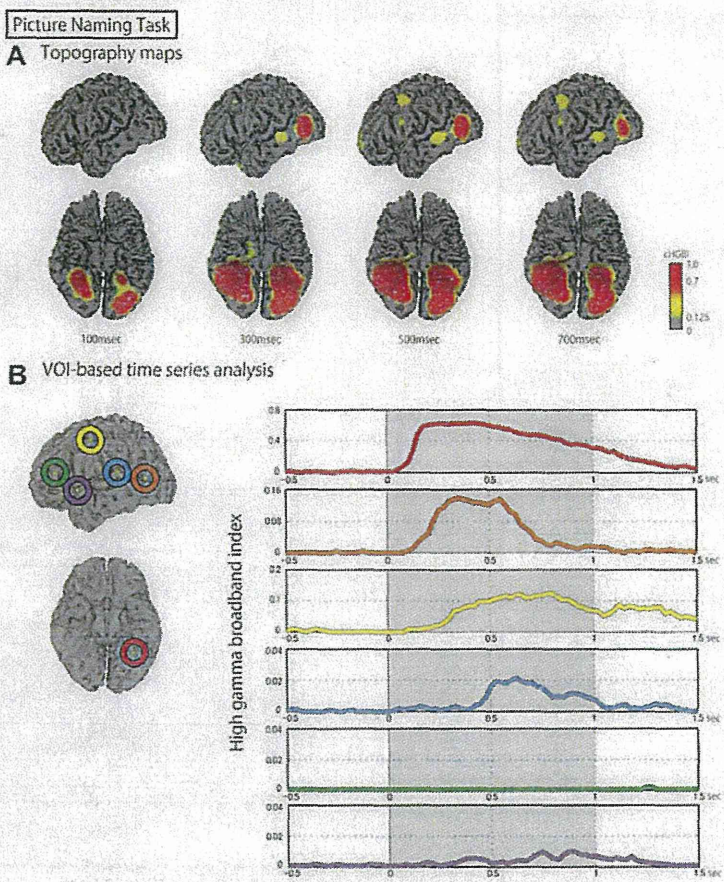

Fig. 4. Picture naming results. The plotting conventions were the same as those employed for Fig. 3. There were marked activations in the bilateral fusiform gyri. The posterior middle temporal gyrus and ventral premotor cortex showed similar dynamics to those observed during the word interpretation task. In contrast to the word interpretation task, the picture naming task induced little activation in the frontal lobe.

served over the MFG-IFG region. The VG task widely activated the STG instead of the FuG between 100 and 600 ms after the presentation of auditory stimuli. The HGA produced in the IFG during the VG task was stronger than those observed during the WI and PN tasks, although similar HGA-propagations were seen in other areas. This report presented a novel technique of ECoG visualization and successfully elucidated typical HGA profiles for different language processes.

Neuroimaging studies have accumulated knowledge about the putative roles of distributed cortical areas. Since WI task used in this study could be achieved only through covertly reading the visually presented words, it seems reasonable to discuss its processing in the context of reading function. In previous studies of the functional areas implicated in word reading, posterior-to-anterior streams of cortical recruitment have generally been described. After the perception of visual stimuli, the FuG is activated during orthographic cognition (Binder et al., 2006; Cohen et al., 2002; Dehaene et al., 2005; Tsapkini and Rapp, 2010). The pMTG is related to lexico-semantic knowledge, and the IFG plays more executive roles in semantic decisions (Badre and Wagner, 2007; Binder et al., 2009; Fiez, 1997; Martin et al., 1995, 1996; Noppeney et al., 2004; Thompson-Schill et al., 1997; Wagner et al., 2001). The WI task used in this study activated these epicenters, and we successfully visualized the sequential activation of each of the abovementioned brain regions. We believe that our findings support the classical model of reading dynamics.

Picture naming is a common language task employed in neurosurgical language mapping (Ojemann et al., 1989; Penfield and Roberts, 1959; Sinai et al., 2005). However, this task did not activate frontal language areas as strongly as categorization or verb generation tasks in fMRI studies (Herholz et al., 1997; Kunii et al., 2011). In general, picture naming has one correct answer. On the contrary, categorization and verb generation tasks require more executive-level semantic judgment or selection (Edwards et al., 2010; Thompson-Schill et al., 1998), which might account for the stronger activation in the frontal language areas. Our results are consistent with this interpretation as the PN task induced little activation in the IFG or MFG in contrast to the WI task. Several previous fMRI studies showed that naming elicited greater cortical activation in the IFG or MFG than word reading task (MacDonald et al., 2000; Polk et al., 2008). Wu et al. directly compared picture naming with word reading task in their ECoG study and found picture naming task demonstrated wider frontal lobe activation (Wu et al., 2011). We assume that the lack of frontal lobe activation in these studies came from passive reading tasks in contrast to our study, which required semantic decision. This suggests that performing the PN task alone in clinical situations carries a risk of underestimating the cortical areas involved in semantic decision-making.

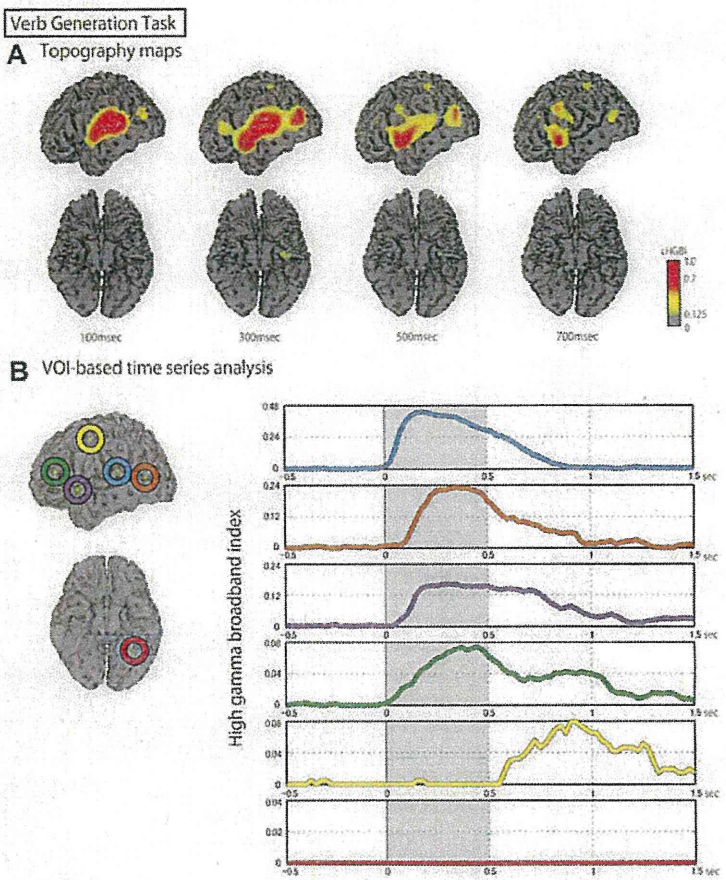

Fig. 5. Verb generation results. The plotting conventions were the same as those employed for Fig. 3. The auditory stimuli resulted in initial activation of the superior temporal gyrus, followed by the recruitment of the posterior middle temporal gyrus. Activation of the ventral premotor cortex occurred later than in the word interpretation and picture naming tasks. The prolonged recruitment observed in the inferior frontal gyrus was as marked as that in the word interpretation task.

In the VG task, our most remarkable finding was the strong activity in the STG and IFG. Several studies have suggested that the STG responds best to the complex spectro-temporal signals, such as speech, that comprise the higher levels of the cortical auditory processing hierarchy (Binder et al., 2000; Hickok and Poeppel, 2004; Scott et al., 2000). As described above, the IFG plays executive roles in semantic decision-making. The VG task involved selecting one of generated words, which might require complex semantic decision-making in the IFG. These task-dependent characteristics might have generated the characteristic activation patterns observed during the VG task.

We observed two cortical areas that were commonly recruited during language processing. The pMTG was activated not only by visual tasks, but also by auditory tasks, soon after the initial integrative perception in the FuG and STG, respectively. This suggests that the pMTG plays a modality-independent role in various semantic processes. It seems quite reasonable that semantic knowledge is stored in the pMTG irrespective of the input modality due to its storage capacity.

The vPMC was also commonly activated by the three tasks. It was suggested that the vPMC might be involved in imagery articulation during silent rehearsal (Vigneau et al., 2006; Wilson et al., 2004), which could be used to ensure that the verbal working memory remains active (Baddeley, 1992; Baddeley and Hitch, 1974; Hickok and Poeppel, 2004). Furthermore, Duffau et al. (2003) suggested that the functional role of the vPMC involved articulation planning by observing language impairment using electrical stimulation of the vPMC. Our results support the assertion that the vPMC plays an important role in basic language functions such as reading, naming, and listening.

Three human ECoG studies have described the HGA dynamics involved in language processing (Canolty et al., 2007; Edwards et al., 2010; Mainy et al., 2008; Pei et al., 2011). Canolty et al. examined 256 subdural electrode channels in 4 epilepsy patients and provided detailed ECoG dynamics for auditory word processing in the temporal lobe. They demonstrated the sequential activation of the posterior STG, middle STG, and superior temporal sulcus, which added temporal information to functional knowledge of these areas gathered by previous studies.

Mainy et al. performed intracranial EEG using 300 depth electrode channels in 10 epilepsy patients. They observed initial gamma-band activation in the mesial basal temporal lobe at 150 ms, which reached the word form area in the mid fusiform gyrus at 200 ms after word reading. Task specific gamma-band activations were then observed after 400 ms in the superior temporal gyrus for both word and pseudo-word stimuli; in the pars triangularis for word categorization and in the pars opercularis for phonological decision-making. Although the brain areas covered by their

study were subject to practical limitations, they successfully demonstrated consistent dynamics in the frontotemporal language areas across individuals. Our study succeeded in superimposing brain activity data from more than 1500 ECoG-channels onto a normalized brain, which demonstrated similar activation patterns, including visual processing in the fusiform gyrus at around 200 ms and semantic processing in the pars triangularis after 400 ms.

Edward et al. investigated 4 patients with ECoG, using auditory verb generation and picture naming tasks. Their individual ECoG analyses clearly showed that in the verb generation task the initial gamma band activation occurred in the pSTG at around 100 ms, before rapidly moving to the pMTG at around 300 ms. After speech perception, activations for semantic processing were detected over the IFG and MFG. It is worth noting that the verb generation task activated the IFG and MFG significantly more than the picture naming task. Despite the limited number of patients in their study, the time course of cortical activation showed close similarities with the HGA dynamics observed in our study. Edward et al. also referred to the contribution made by the vPMC to speech perception. We strongly agree that the vPMC plays an important role in language tasks.

Pei et al. recently reported spatiotemporal dynamics of ECoG HGA during overt and covert word repetition. Although the investigation was limited to the lateral parasylvian area, they projected each electrodes from 8 subjects onto the template brain for the first time and presented comprehensive characterization of overt and covert speech. They also related the results to the temporal envelope of auditory stimulation and the subject's verbal response. Their study reinforced the important role of HGA as a general index of cortical activation.

The novel achievement of this study was that we were able to normalize all of the ECoG electrode positions of the 21 patients, thereby avoiding inter-individual variability in the obtained spatial and temporal ECoG profiles. Although we acknowledge that this method carries a risk of underestimating weak and inconsistent HGA, it emphasizes the prominent hot spots related to language processing and is helpful for understanding the mechanisms underlying language functions. It is important to note that the spatial comparison of this study was not statistically validated, which implies spatially non-stationary correlation structure of the observed activity. It would be necessary to address the methodological issue for future studies.

In this study, we observed little activation in the angular gyrus or anterior temporal area even though they are considered to be language related areas. Both areas have been suggested to play a role in integrating individual concepts into a larger whole and in sentence-level comprehension (Friederici et al., 2003; Hickok and Poeppel, 2007; Humphries et al., 2001; Newman et al., 2003; Ni et al., 2000). In this report, we made the tasks as easy as possible, since single object processing might be appropriate for functional normalization among patients with a variety of attention levels. In order to identify additional language areas, we might need to use more complex tasks such as sentence comprehension. On the other hand, the anterior medial temporal region seems to show HGA augmentation at around 300 ms in WI and PN tasks. Given that such augmentation was not observed in VG task; this could be attributed to artifacts elicited by fixational eye movements (Nagasawa et al., 2011; Yuval-Greenberg et al., 2008).

Electrode shifts are one of the crucial issues affecting ECoG research (Laviolette et al., 2011). Estimation errors related to electrode localization are also inevitable at each step of normalization, digitization, and registration. In our study, we confirmed the electrode locations in the 2nd operation and that the normalized electrodes produced using SPM8 uniformly covered the language-related areas. As a result, a large number of the electrodes (more than 1500 channels) showed representative HGA dynamics for each semantic task, which suggests that this method has great potential for improving our understanding of the underlying physiology supporting language functions. Another issue is the reference electrode position, that is Cz in all patients. Thus, high-gamma activity generated by the superior midline region on either hemisphere might contaminate ECoG data at all channels (Brown et al., 2008; Koga et al., 2011). In addition, although we checked all patients achieved the semantic tasks before investigations, neither behavioral performance nor response time was measured during ECoG recordings to avoid contamination of motor responses. Therefore, it was difficult to determine the HGA augmentation according to the response onset. Finally, the occipital pole or the medial surface of cortex was not sampled in the present study. Some ECoG studies previously showed the spatial–temporal characteristics of HGA augmentation involving these areas; thus these studies might supplement the weakness of this study (Brown et al., 2008; Wu et al., 2011).

We believe that our ECoG-normalization method is a novel and unique technique and can be used to provide information regarding human brain dynamics, which have been gradually unveiled by numerous previous language studies involving lesion-based and non-invasive imaging approaches.

Acknowledgements

This work was supported in part by the Japan Epilepsy Research Foundation, a grant from the Suhara Memorial Foundation, Grant-in-Aid No. 24390337 for Scientific Research (B) from the ministry of Education, Culture, Sports, Science and Technology of Japan (MEXT), Grant-in-Aid No. 23659679 for Challenging Exploratory Research from MEXT, Grant-in-Aid No. 23119701 for Scientific Research on Innovative Areas, "Face perception and recognition" from MEXT, and a Research Grant for "Decoding and controlling brain-information" from the Japan Science and Technology Agency.

References

Axmacher N, Mormann F, Fernandez G, Cohen MX, Elger CE, Fell J. Sustained neural activity patterns during working memory in the human medial temporal lobe. J Neurosci 2007;27:7807–16.
Baddeley A. Working memory. Science 1992;255:556–9.
Baddeley A, Hitch G. Working memory. In: Bower GH, editor. The psychology of learning and motivation. San Diego: Academic Press; 1974. p. 47–90.
Badre D, Wagner AD. Left ventrolateral prefrontal cortex and the cognitive control of memory. Neuropsychologia 2007;45:2883–901.
Benjamini Y, Hochberg Y. Controlling the false discovery rate – a practical and powerful approach to multiple testing. J Roy Statist Soc Ser B 1995;57:289–300.
Binder JR, Desai RH, Graves WW, Conant LL. Where is the semantic system? A critical review and meta-analysis of 120 functional neuroimaging studies. Cereb Cortex 2009;19:2767–96.
Binder JR, Frost JA, Hammeke TA, Bellgowan PS, Springer JA, Kaufman JN, et al. Human temporal lobe activation by speech and nonspeech sounds. Cereb Cortex 2000;10:512–28.
Binder JR, Medler DA, Westbury CF, Liebenthal E, Buchanan L. Tuning of the human left fusiform gyrus to sublexical orthographic structure. Neuroimage 2006;33:739–48.
Brown EC, Rothermel R, Nishida M, Juhasz C, Muzik O, Hoechstetter K, et al. In vivo animation of auditory-language-induced gamma-oscillations in children with intractable focal epilepsy. Neuroimage 2008;41:1120–31.
Buchsbaum BR, Hickok G, Humphries C. Role of left posterior superior temporal gyrus in phonological processing for speech perception and production. Cogn Sci 2001;25:663–78.
Canolty RT, Soltani M, Dalal SS, Edwards E, Dronkers NF, Nagarajan SS, et al. Spatiotemporal dynamics of word processing in the human brain. Front Neurosci 2007;1:185–96.
Champod AS, Petrides M. Dissociable roles of the posterior parietal and the prefrontal cortex in manipulation and monitoring processes. Proc Natl Acad Sci USA 2007;104:14837–42.
Champod AS, Petrides M. Dissociation within the frontoparietal network in verbal working memory: a parametric functional magnetic resonance imaging study. J Neurosci 2010;30:3849–56.
Cohen L, Lehericy S, Chochon F, Lemer C, Rivaud S, Dehaene S. Language-specific tuning of visual cortex? Functional properties of the Visual Word Form Area. Brain 2002;125:1054–69.

Crone NE, Boatman D, Gordon B, Hao L. Induced electrocorticographic gamma activity during auditory perception. Brazier Award-winning article, 2001. Clin Neurophysiol 2001a;112:565–82.
Crone NE, Hao L, Hart Jr J, Boatman D, Lesser RP, Irizarry R, et al. Electrocorticographic gamma activity during word production in spoken and sign language. Neurology 2001b;57:2045–53.
Crone NE, Miglioretti DL, Gordon B, Lesser RP. Functional mapping of human sensorimotor cortex with electrocorticographic spectral analysis. II. Event-related synchronization in the gamma band. Brain 1998;121(Pt 12):2301–15.
Curran T, Tucker DM, Kutas M, Posner MI. Topography of the N400: brain electrical activity reflecting semantic expectancy. Electroencephalogr Clin Neurophysiol 1993;88:188–209.
D'Ausilio A, Pulvermuller F, Salmas P, Bufalari I, Begliomini C, Fadiga L. The motor somatotopy of speech perception. Curr Biol 2009;19:381–5.
Dehaene S, Cohen L, Sigman M, Vinckier F. The neural code for written words: a proposal. Trends Cogn Sci 2005;9:335–41.
Dhond RP, Witzel T, Dale AM, Halgren E. Spatiotemporal cortical dynamics underlying abstract and concrete word reading. Hum Brain Mapp 2007;28:355–62.
Dronkers NF, Wilkins DP, Van Valin Jr RD, Redfern BB, Jaeger JJ. Lesion analysis of the brain areas involved in language comprehension. Cognition 2004;92:145–77.
Duffau H, Capelle L, Denvil D, Gatignol P, Sichez N, Lopes M, et al. The role of dominant premotor cortex in language: a study using intraoperative functional mapping in awake patients. Neuroimage 2003;20:1903–14.
Edwards E, Nagarajan SS, Dalal SS, Canolty RT, Kirsch HE, Barbaro NM, et al. Spatiotemporal imaging of cortical activation during verb generation and picture naming. Neuroimage 2010;50:291–301.
Edwards E, Soltani M, Deouell LY, Berger MS, Knight RT. High gamma activity in response to deviant auditory stimuli recorded directly from human cortex. J Neurophysiol 2005;94:4269–80.
Fiez JA. Phonology, semantics, and the role of the left inferior prefrontal cortex. Hum Brain Mapp 1997;5:79–83.
Friederici AD, Ruschemeyer SA, Hahne A, Fiebach CJ. The role of left inferior frontal and superior temporal cortex in sentence comprehension: localizing syntactic and semantic processes. Cereb Cortex 2003;13:170–7.
Genovese CR, Lazar NA, Nichols T. Thresholding of statistical maps in functional neuroimaging using the false discovery rate. Neuroimage 2002;15:870–8.
Halgren E, Dhond RP, Christensen N, Van Petten C, Marinkovic K, Lewine JD, et al. N400-like magnetoencephalography responses modulated by semantic context, word frequency, and lexical class in sentences. Neuroimage 2002;17:1101–16.
Hashimoto R, Sakai KL. Specialization in the left prefrontal cortex for sentence comprehension. Neuron 2002;35:589–97.
Helenius P, Salmelin R, Service E, Connolly JF. Distinct time courses of word and context comprehension in the left temporal cortex. Brain 1998;121(Pt 6):1133–42.
Herholz, K., Reulen, H.J., von Stockhausen, H.M., Thiel, A., Ilmberger, J., Kessler, J., et al. Preoperative activation and intraoperative stimulation of language-related areas in patients with glioma. Neurosurgery 1997; 41: 1253–1260; discussion 1260–1252.
Hickok G. Functional anatomy of speech perception and speech production: psycholinguistic implications. J Psycholinguist Res 2001;30:225–35.
Hickok G, Buchsbaum B, Humphries C, Muftuler T. Auditory-motor interaction revealed by fMRI: speech, music, and working memory in area Spt. J Cogn Neurosci 2003;15:673–82.
Hickok G, Poeppel D. Dorsal and ventral streams: a framework for understanding aspects of the functional anatomy of language. Cognition 2004;92:67–99.
Hickok G, Poeppel D. The cortical organization of speech processing. Nat Rev Neurosci 2007;8:393–402.
Homae F, Hashimoto R, Nakajima K, Miyashita Y, Sakai KL. From perception to sentence comprehension: the convergence of auditory and visual information of language in the left inferior frontal cortex. Neuroimage 2002;16:883–900.
Homae F, Yahata N, Sakai KL. Selective enhancement of functional connectivity in the left prefrontal cortex during sentence processing. Neuroimage 2003;20:578–86.
Howard MW, Rizzuto DS, Caplan JB, Madsen JR, Lisman J, Aschenbrenner-Scheibe R, et al. Gamma oscillations correlate with working memory load in humans. Cereb Cortex 2003;13:1369–74.
Humphries C, Willard K, Buchsbaum B, Hickok G. Role of anterior temporal cortex in auditory sentence comprehension: an fMRI study. Neuroreport 2001;12:1749–52.
Johnson BW, Hamm JP. High-density mapping in an N400 paradigm: evidence for bilateral temporal lobe generators. Clin Neurophysiol 2000;111:532–45.
Jonides J, Schumacher EH, Smith EE, Koeppe RA, Awh E, Reuter-Lorenz PA, et al. The role of parietal cortex in verbal working memory. J Neurosci 1998;18:5026–34.
Jung J, Mainy N, Kahane P, Minotti L, Hoffmann D, Bertrand O, et al. The neural bases of attentive reading. Hum Brain Mapp 2008;29:1193–206.
Kamada K, Sawamura Y, Takeuchi F, Kuriki S, Kawai K, Morita A, et al. Expressive and receptive language areas determined by a non-invasive reliable method using functional magnetic resonance imaging and magnetoencephalography. Neurosurgery 2007;60:296–305.
Koga S, Rothermel R, Juhasz C, Nagasawa T, Sood S, Asano E. Electrocorticographic correlates of cognitive control in a Stroop task-intracranial recording in epileptic patients. Hum Brain Mapp 2011;32:1580–91.
Kunii, N., Kamada, K., Ota, T., Kawai, K., Saito, N. A detailed analysis of functional magnetic resonance imaging in the frontal language area - a comparative study with extraoperative electrocortical stimulation. Neurosurgery 2011; 69: 590–596; discussion 596–597.
Lachaux JP, George N, Tallon-Baudry C, Martinerie J, Hugueville L, Minotti L, et al. The many faces of the gamma band response to complex visual stimuli. Neuroimage 2005;25:491–501.
Laviolette PS, Rand SD, Ellingson BM, Raghavan M, Lew SM, Schmainda KM, et al. 3D visualization of subdural electrode shift as measured at craniotomy reopening. Epilepsy Res 2011;94:102–9.
Leuthardt, E.C., Miller, K., Anderson, N.R., Schalk, G., Dowling, J., Miller, J., et al. Electrocorticographic frequency alteration mapping: a clinical technique for mapping the motor cortex. Neurosurgery 2007; 60: 260–270; discussion 270–261.
MacDonald III AW, Cohen JD, Stenger VA, Carter CS. Dissociating the role of the dorsolateral prefrontal and anterior cingulate cortex in cognitive control. Science 2000;288:1835–8.
Maess B, Herrmann CS, Hahne A, Nakamura A, Friederici AD. Localizing the distributed language network responsible for the N400 measured by MEG during auditory sentence processing. Brain Res 2006;1096:163–72.
Mainy N, Jung J, Baciu M, Kahane P, Schoendorff B, Minotti L, et al. Cortical dynamics of word recognition. Hum Brain Mapp 2008;29:1215–30.
Makeig S. Auditory event-related dynamics of the EEG spectrum and effects of exposure to tones. Electroencephalogr Clin Neurophysiol 1993;86:283–93.
Martin A, Haxby JV, Lalonde FM, Wiggs CL, Ungerleider LG. Discrete cortical regions associated with knowledge of color and knowledge of action. Science 1995;270:102–5.
Martin A, Wiggs CL, Ungerleider LG, Haxby JV. Neural correlates of category-specific knowledge. Nature 1996;379:649–52.
Meltzer JA, Zaveri HP, Goncharova II, Distasio MM, Papademetris X, Spencer SS, et al. Effects of working memory load on oscillatory power in human intracranial EEG. Cereb Cortex 2008;18:1843–55.
Miller KJ, Leuthardt EC, Schalk G, Rao RP, Anderson NR, Moran DW, et al. Spectral changes in cortical surface potentials during motor movement. J Neurosci 2007;27:2424–32.
Moore CJ, Price CJ. A functional neuroimaging study of the variables that generate category-specific object processing differences. Brain 1999;122(Pt 5):943–62.
Nagasawa T, Matsuzaki N, Juhasz C, Hanazawa A, Shah A, Mittal S, et al. Occipital gamma-oscillations modulated during eye movement tasks: simultaneous eye tracking and electrocorticography recording in epileptic patients. Neuroimage 2011;58:1101–9.
Newman SD, Just MA, Keller TA, Roth J, Carpenter PA. Differential effects of syntactic and semantic processing on the subregions of Broca's area. Brain Res Cogn Brain Res 2003;16:297–307.
Ni W, Constable RT, Mencl WE, Pugh KR, Fulbright RK, Shaywitz SE, et al. An event-related neuroimaging study distinguishing form and content in sentence processing. J Cogn Neurosci 2000;12:120–33.
Noppeney U, Josephs O, Kiebel S, Friston KJ, Price CJ. Action selectivity in parietal and temporal cortex. Brain Res Cogn Brain Res 2005;25:641–9.
Noppeney U, Phillips J, Price C. The neural areas that control the retrieval and selection of semantics. Neuropsychologia 2004;42:1269–80.
Ojemann G, Ojemann J, Lettich E, Berger M. Cortical language localization in left, dominant hemisphere. An electrical stimulation mapping investigation in 117 patients. J Neurosurg 1989;71:316–26.
Ossadtchi A, Greenblatt RE, Towle VL, Kohrman MH, Kamada K. Inferring spatiotemporal network patterns from intracranial EEG data. Clin Neurophysiol 2010;121:823–35.
Pei X, Leuthardt EC, Gaona CM, Brunner P, Wolpaw JR, Schalk G. Spatiotemporal dynamics of electrocorticographic high gamma activity during overt and covert word repetition. Neuroimage 2011;54:2960–72.
Penfield W, Roberts L. Speech and brain-mechanisms. Princeton, NJ: Princeton University Press; 1959.
Pfurtscheller G, Lopes da Silva FH. Event-related EEG/MEG synchronization and desynchronization: basic principles. Clin Neurophysiol 1999;110:1842–57.
Polk TA, Drake RM, Jonides JJ, Smith MR, Smith EE. Attention enhances the neural processing of relevant features and suppresses the processing of irrelevant features in humans: a functional magnetic resonance imaging study of the Stroop task. J Neurosci 2008;28:13786–92.
Price CJ. The anatomy of language: a review of 100 fMRI studies published in 2009. Ann NY Acad Sci 2010;1191:62–88.
Pulvermuller F, Huss M, Kherif F, Moscoso del Prado Martin F, Hauk O, Shtyrov Y. Motor cortex maps articulatory features of speech sounds. Proc Natl Acad Sci USA 2006;103:7865–70.
Pylkkanen L, McElree B. An MEG study of silent meaning. J Cogn Neurosci 2007;19:1905–21.
Rauschecker JP. Cortical processing of complex sounds. Curr Opin Neurobiol 1998;8:516–21.
Ravizza SM, Delgado MR, Chein JM, Becker JT, Fiez JA. Functional dissociations within the inferior parietal cortex in verbal working memory. Neuroimage 2004;22:562–73.
Ray S, Niebur E, Hsiao SS, Sinai A, Crone NE. High-frequency gamma activity (80–150 Hz) is increased in human cortex during selective attention. Clin Neurophysiol 2008;119:116–33.
Salmelin R, Hari R, Lounasmaa OV, Sams M. Dynamics of brain activation during picture naming. Nature 1994;368:463–5.
Scott SK, Blank CC, Rosen S, Wise RJ. Identification of a pathway for intelligible speech in the left temporal lobe. Brain 2000;123(Pt 12):2400–6.

Sederberg PB, Schulze-Bonhage A, Madsen JR, Bromfield EB, McCarthy DC, Brandt A, et al. Hippocampal and neocortical gamma oscillations predict memory formation in humans. Cereb Cortex 2007;17:1190–6.
Sinai A, Bowers CW, Crainiceanu CM, Boatman D, Gordon B, Lesser RP, et al. Electrocorticographic high gamma activity versus electrical cortical stimulation mapping of naming. Brain 2005;128:1556–70.
Sinai A, Crone NE, Wied HM, Franaszczuk PJ, Miglioretti D, Boatman-Reich D. Intracranial mapping of auditory perception: event-related responses and electrocortical stimulation. Clin Neurophysiol 2009;120:140–9.
Tallon-Baudry C, Bertrand O, Henaff MA, Isnard J, Fischer C. Attention modulates gamma-band oscillations differently in the human lateral occipital cortex and fusiform gyrus. Cereb Cortex 2005;15:654–62.
Tanji K, Suzuki K, Delorme A, Shamoto H, Nakasato N. High-frequency gamma-band activity in the basal temporal cortex during picture-naming and lexical-decision tasks. J Neurosci 2005;25:3287–93.
Thompson-Schill SL, D'Esposito M, Aguirre GK, Farah MJ. Role of left inferior prefrontal cortex in retrieval of semantic knowledge: a reevaluation. Proc Natl Acad Sci USA 1997;94:14792–7.
Thompson-Schill SL, D'Esposito M, Kan IP. Effects of repetition and competition on activity in left prefrontal cortex during word generation. Neuron 1999;23:513–22.
Thompson-Schill SL, Swick D, Farah MJ, D'Esposito M, Kan IP, Knight RT. Verb generation in patients with focal frontal lesions: a neuropsychological test of neuroimaging findings. Proc Natl Acad Sci USA 1998;95:15855–60.
Trautner P, Rosburg T, Dietl T, Fell J, Korzyukov OA, Kurthen M, et al. Sensory gating of auditory evoked and induced gamma band activity in intracranial recordings. Neuroimage 2006;32:790–8.
Tsapkini K, Rapp B. The orthography-specific functions of the left fusiform gyrus: evidence of modality and category specificity. Cortex 2010;46:185–205.
Tse CY, Lee CL, Sullivan J, Garnsey SM, Dell GS, Fabiani M, et al. Imaging cortical dynamics of language processing with the event-related optical signal. Proc Natl Acad Sci USA 2007;104:17157–62.
Tsukiura T, Fujii T, Takahashi T, Xiao R, Inase M, Iijima T, et al. Neuroanatomical discrimination between manipulating and maintaining processes involved in verbal working memory; a functional MRI study. Brain Res Cogn Brain Res 2001;11:13–21.
Uusvuori J, Parviainen T, Inkinen M, Salmelin R. Spatiotemporal interaction between sound form and meaning during spoken word perception. Cereb Cortex 2008;18:456–66.
van Vugt MK, Schulze-Bonhage A, Litt B, Brandt A, Kahana MJ. Hippocampal gamma oscillations increase with memory load. J Neurosci 2010;30:2694–9.
Vartiainen J, Parviainen T, Salmelin R. Spatiotemporal convergence of semantic processing in reading and speech perception. J Neurosci 2009;29:9271–80.
Vigneau M, Beaucousin V, Herve PY, Duffau H, Crivello F, Houde O, et al. Meta-analyzing left hemisphere language areas: phonology, semantics, and sentence processing. Neuroimage 2006;30:1414–32.
Wagner AD, Pare-Blagoev EJ, Clark J, Poldrack RA. Recovering meaning: left prefrontal cortex guides controlled semantic retrieval. Neuron 2001;31:329–38.
Wilson SM, Saygin AP, Sereno MI, Iacoboni M. Listening to speech activates motor areas involved in speech production. Nat Neurosci 2004;7:701–2.
Wu HC, Nagasawa T, Brown EC, Juhasz C, Rothermel R, Hoechstetter K, et al. Gamma-oscillations modulated by picture naming and word reading: intracranial recording in epileptic patients. Clin Neurophysiol 2011;122:1929–42.
Wu M, Wisneski K, Schalk G, Sharma M, Roland J, Breshears J, et al. Electrocorticographic frequency alteration mapping for extraoperative localization of speech cortex. Neurosurgery 2010;66:E407–9.
Yuval-Greenberg S, Tomer O, Keren AS, Nelken I, Deouell LY. Transient induced gamma-band response in EEG as a manifestation of miniature saccades. Neuron 2008;58:429–41.
Zygierewicz J, Durka PJ, Klekowicz H, Franaszczuk PJ, Crone NE. Computationally efficient approaches to calculating significant ERD/ERS changes in the time-frequency plane. J Neurosci Methods 2005;145:267–76.

てんかんに対する迷走神経刺激療法の実施ガイドライン

川合謙介*
日本てんかん学会ガイドライン作成委員会
委員長 須貝研司
委 員 赤松直樹、岡崎光俊、亀山茂樹、笹川睦男、辻 貞俊、前原健寿、山本 仁
*東京大学大学院医学系研究科

1. はじめに

迷走神経刺激療法 vagus nerve stimulation (VNS) は、てんかんに対する非薬剤治療のひとつであり、抗てんかん薬に抵抗する難治性てんかん発作を減少、軽減する緩和的治療である。植込型の電気刺激装置により、左頸部迷走神経を間歇的に刺激する。欧米では1990年代から行われており、わが国でも2010年7月から保険適用となった。

VNSは本邦初のてんかんに対する植込型装置による電気刺激療法であり、治療適応や施行方法についての混乱を避けるため、日本てんかん学会としてのガイドラインを提示する。

2. VNSの目的

Q. VNSは効果があるか？

VNSは薬剤抵抗性てんかん発作に対して緩和効果がある。【推奨度 A】

解説

VNSの治療対象は薬剤抵抗性のてんかん発作であり、てんかん発作の緩和を目的に施行する[1,2]。VNSはあくまで緩和的治療であり、発作の完全消失を目指すものではない。てんかん発作の緩和効果の他に、てんかん患者にみられる認知機能障害・悄動障害などの随伴症状に対する有効性が報告されているが[3-6]、これらはてんかん発作に対して施行されたVNSを利用した研究であり、随伴症状に対する効果を主目的としたstudy designとしては十分なものではない。したがって、随伴症状の軽減を主目的とする治療適応を支持する十分な科学的根拠とはならない。

3. VNSの対象患者

Q. VNSはどのような患者とてんかん発作が対象となるか？

薬剤抵抗性のてんかん発作で開頭手術の対象とならない発作【推奨度 C】

解説

VNSの有効性は、米国で行われた12歳以上の部分発作を対象とする二つの無作為対照試験で検証された[1,2]。これらの試験では、治療3ヶ月での強刺激群と弱刺激群における平均発作減少率は各々25-28%、6-15%であった。

一方、小児や全般発作に対する無作為対照試験は行われていない。しかし、多くの症例シリーズ研究で有効性が報告されている[6-8]。したがって、小児や全般発作に対して使用する場合は慎重に適応を判断し、治療開始後も有効性と有害事象に関する追跡調査を行う必要がある。本邦では薬事承認の際に厚生労働省から、12歳未満の小児全例での使用成績調査が義務付けられた。

4. VNSの長期効果と有効性の判定

Q. VNSの長期発作抑制効果は期待できるか？　また無効と判断するまでにどの程度の期間、治療を継続するべきか？

1. VNSの発作抑制率は治療継続によりおよそ2年間増大し、その後安定して継続すると期待できる。【推奨度C】
2. VNSが無効と判断するまでに2年間は治療を継続する。【推奨度C】

解説

前項で取り上げた二つの無作為対照試験の治療期間は3ヶ月と短かったが、その後のオープンラベル追跡調査により、発作が50%以上減少する患者の率は、治療期間1年で37%、2年43%、3年43%と、年単位での治療継続で徐々に発作抑制効果が徐々に高まり、発作減少率はおよそ50%で安定する[9,10]。なお、年齢や発作型あるいはてんかん分類によって長期成績に大きな差はみられていない[9,10]。

VNSを無効と判断する基準に関する研究報告はないが、上記の長期治療効果の報告から、2年間は治療の継続が必要と考えられる。

5. VNSの術前検査

Q. VNS施行前にはどのような検査が必要か？

根治的な開頭手術の適否を精査した上で、VNSの適応を判断する。【推奨度C】

解説

VNSの適応判断には、開頭手術の術前精査に準じた検査を行う。VNSのてんかん発作に対する効果は緩和的であり、開頭による焦点切除術に根治的効果が期待できる場合は、原則的に開頭手術の施行を検討するべきである。ビデオ脳波などの基本的な術前検査を省略したため、適応外の患者にVNSが行われたという報告もある[11]。

6. VNS刺激装置の植込手術

Q. VNSに用いる刺激装置の植込手術はどのように行うか。

VNSには専用の植込型刺激装置システムを用いる。装置の植込手術は、原則的に全身麻酔下で行い、パルスジェネレータを左前胸部皮下脂肪層に、らせん電極を左迷走神経に留置する。【推奨度C】

解説

装置の植込手術は、製造元が作成した専用の埋込型刺激装置システムのマニュアルに従って行う。試験刺激中の一過性徐脈・心停止（0.2%）や術後一過性の反回神経麻痺（1%）など手術合併症を避けるため、適切な部位での迷走神経確保や愛護的な電極留置操作を行う[12]。

パルスジェネレータの電源寿命は現在のところ約6年で、治療継続のためにはパルスジェネレータの交換手術が必要である。電源寿命による装置停止による発作の再発や悪化があり得るので、製造元マニュアルに従った定期的なデバイス診断により予想残存寿命を確認し、装置停止前に警告に従ってパルスジェネレータを交換する[13,14]。

7. VNS治療の方法

Q. VNSの刺激治療はどのように行うか。

VNSは、原則として植込手術の2週間後から開始する。弱い刺激強度から開始し、副作用の発現に注意しながら徐々に刺激強度を上げる。【推奨度C】

解説

刺激治療は装置植込の約2週間後から開始する。標準的には、0.25 mA、500 usec、30 Hz、30秒ON、5分

OFF、で開始し、副作用の出現しない範囲で、発作に対する効果をみながら最大3.50 mAまで上げてゆく[15]。効果がなければ、duty cycle（1サイクルのうちON時間の占める割合）も上げてゆく。至適条件は患者によって異なり、試行錯誤が必要である[15,16]。

8. VNSの副作用

Q. 刺激開始時の副作用はどのようなものがあり、どう対応するか。

VNS刺激開始時の副作用は、咳、嗄声、咽頭部不快感、嚥下障害などである。忍容できない副作用には刺激強度を下げることで対応する。【推奨度C】

解説

刺激治療に伴う副作用は、咳、嗄声、咽頭部不快感、嚥下障害などだが、これらは可逆的で、忍容できない副作用には刺激強度を下げて対応する。副作用の発現率は治療継続とともに減少する[29]。突然の動作不良など緊急時には、製造元マニュアルに従って装置を緊急停止させ、直ちに条件設定の可能な医療施設を受診させる。

9. VNSと医療機器・電気電子機器との相互作用

Q. VNSと医療機器・電気電子機器との相互作用は問題にならないか？ 特にMRIについてはどうか？

1. VNS治療中の患者における頭部MRI検査は、頭部撮像に限り製造元マニュアルに従って施行可能である。【推奨度C】 2. 日常生活における電気電子機器からの影響は最小限のものだが、強い磁場からは15 cm以上離れる。【推奨度C】

解説

VNS治療中の患者に対するMRI検査は、3テスラ以下（3テスラを含む）の頭部コイルを用いた頭部撮像に限り、刺激を中断し製造元マニュアルの推奨条件下に施行可能である[17]。

脳磁図は安全に施行できるが、ノイズ対策が必要である[18,19]。

家電製品、携帯電話、空港の金属探知機や商店の盗難防止センサーなどからはVNS装置は影響を受けない。ただし、非常に強い磁石は刺激開始や中止の誤指令を出す可能性があり、製造元のマニュアルでは、大きなスピーカーやバイブレーターなど強い磁石を内蔵する機器からは15 cm以上離れるよう推奨している。

10. 効果がないと判断する場合

Q. VNSが無効と判断した場合の対処方法は？

1. 忍容範囲で刺激条件を最大まで上げ、または2年以上の継続治療を行った上で無効と判断された場合、刺激を停止し、てんかん発作の経過を観察する。【推奨度C】 2. 患者または家族の希望により装置の抜去を検討する。【推奨度C】

解説

発作と他の症状への効果より総合的にVNSが無効と判断した場合の対処方法に関する研究報告はないが、刺激を停止することを考慮する。一方、パルスジェネレータの電源寿命が尽きた患者では、てんかん発作の悪化があり得る[13,14]。したがって、刺激条件を下げた場合、停止した場合には、てんかん発作の悪化がないか経過観察を行う。

患者・家族が希望すれば装置の抜去を検討する。VNS装置抜去手術のリスクに関する研究報告はないが、パルスジェネレータ抜去手術の合併症発生率はきわめて低いと予想される。一方、迷走神経に留置した電極の抜去手術は、電極と神経の癒着から、神経損傷の相応なリスクを有するが[20]、安全な抜去が可能との報告もある[21]。

11. その他

Q. VNS施行についてその他の留意事項は何か？

本治療の施行に際しては、てんかん診療に関する十分な知識と経験を有するてんかん専門医が、技術講習会を受講し、迷走神経刺激療法資格認定委員会による認定を受けた後に施行する（日本てんかん学会、日本てんかん外科学会、日本脳外科学会合同の迷走刺激療法認定委員会によるガイドラインを参照のこと）

解説

承認にあたり、3学会ガイドラインが策定された。日本でVNSを施行する場合にはこれに準拠することが望ましい。ただし、これは3年間で見直すことになっており、変更される可能性がある。

参考　平成22年1月8日薬事承認時に認定委員会によって策定されたガイドライン

1. 本療法の適応判断と刺激装置植込術は、日本てんかん学会専門医ならびに日本脳神経外科学会専門医の両資格を有するてんかん外科治療を専門的に行っている医師によって、またはその指導の下に行われるべきものとする。
2. 本療法の開始後の刺激条件の調整や、治療効果および有害事象の追跡調査は、日本てんかん学会専門医（すべての診療科を含む）またはその指導の下に行われるべきものとする。
3. 本療法を行う医師（1項、2項に該当する医師）は、初回施行前に、日本てんかん学会、日本てんかん外科学会、日本脳神経外科学会の共催による講習会を受講しなければならない。
4. 刺激装置植込術を行う医師は、受講資格として前年1年間のてんかん外科手術症例リストの申告を必要とする。
5. 受講修了者は、3学会合同の認定委員会によって認定証が授与され、本療法の実施資格が認められる。なお、認定は認定委員会によって見直される場合がある。

参考　平成22年1月8日薬事法承認における目的・効果・承認条件

使用目的、効能又は効果

迷走神経刺激装置VNSシステムは、薬剤抵抗性の難治性てんかん発作を有するてんかん患者（開頭手術が奏功する症例を除く）の発作頻度を軽減する補助療法として、迷走神経を刺激する電気刺激装置である。

承認条件

1. てんかん治療に対する十分な知識・経験を有する医師が、難治性てんかん発作に対する本品を用いた迷走神経刺激治療に関する講習の受講等により、本品の有効性及び安全性を十分に理解し、手技及び当該治療に伴う合併症等に関する十分な知識・経験を得た上で、適応を遵守して用いるように必要な措置を講じること。
2. 使用成績調査により、登録症例（国内治験症例を含む。）及び全ての小児症例の長期予後について、経年解析結果を報告するとともに、必要により適切な措置を講じること。

文　献

1) The Vagus Nerve Stimulation Study Group. A randomized controlled trial of chronic vagus nerve stimulation for treatment of medically intractable seizures. The Vagus Nerve Stimulation Study Group. Neurology 1995; 45: 224-30. [I]
2) Handforth A, DeGiorgio CM, Schachter SC, Uthman BM, Naritoku DK, Tecoma ES, Henry TR, Collins SD, Vaughn BV, Gilmartin RC, Labar DR, Morris GL, 3rd, Salinsky MC, Osorio I, Ristanovic RK, Labiner DM, Jones JC, Murphy JV, Ney GC, Wheless JW. Vagus nerve stimulation therapy for partial-onset seizures: a randomized active-control trial. Neurology 1998; 51: 48-55. [I]
3) Clark KB, Naritoku DK, Smith DC, Browning RA, Jensen RA. Enhanced recognition memory following vagus nerve stimulation in human subjects. Nat Neurosci 1999; 2: 94-8. [I]
4) Elger G, Hoppe C, Falkai P, Rush AJ, Elger CE. Vagus nerve stimulation is associated with mood improvements in epilepsy patients. Epilepsy Res 2000; 42: 203-10. [II]
5) Harden CL, Pulver MC, Ravdin LD, Nikolov B, Halper JP, Labar DR. A Pilot Study of Mood in Epilepsy Patients

Treated with Vagus Nerve Stimulation. Epilepsy Behav 2000; 1: 93-99. [II]
6) Murphy JV. Left vagal nerve stimulation in children with medically refractory epilepsy. The Pediatric VNS Study Group. J Pediatr 1999; 134: 563-6. [III]
7) Blount JP, Tubbs RS, Kankirawatana P, Kiel S, Knowlton R, Grabb PA, Bebin M. Vagus nerve stimulation in children less than 5 years old. Childs Nerv Syst 2006; 22: 1167-9. [III]
8) Elliott RE, Rodgers SD, Bassani L, Morsi A, Geller EB, Carlson C, Devinsky O, Doyle WK. Vagus nerve stimulation for children with treatment-resistant epilepsy: a consecutive series of 141 cases. J Neurosurg Pediatr 2011; 7: 491-500. [III]
9) Morris GL, 3rd, Mueller WM. Long-term treatment with vagus nerve stimulation in patients with refractory epilepsy. The Vagus Nerve Stimulation Study Group E01-E05. Neurology 1999; 53: 1731-5. [III]
10) Elliott RE, Morsi A, Tanweer O, Grobelny B, Geller E, Carlson C, Devinsky O, Doyle WK. Efficacy of vagus nerve stimulation over time: review of 65 consecutive patients with treatment-resistant epilepsy treated with VNS > 10 years. Epilepsy Behav 2011; 20: 478-83. [III]
11) Attarian H, Dowling J, Carter J, Gilliam F. Video EEG monitoring prior to vagal nerve stimulator implantation. Neurology 2003; 61: 402-3. [IV]
12) DeGiorgio CM, Amar A, Apuzzo MLJ, Surgical anatomy, implantation technique, and operative complications. In: Vagus Nerve Stimulation. Vol., S.C. Schachter, D. Schmidt, ed. Martin Dunitz Ltd, London; 2001: pp. 31-50. [IV]
13) Tatum WOt, Ferreira JA, Benbadis SR, Heriaud LS, Gieron M, Rodgers-Neame NT, Vale FL. Vagus nerve stimulation for pharmacoresistant epilepsy: clinical symptoms with end of service. Epilepsy Behav 2004; 5: 128-32. [III]
14) Vonck K, Dedeurwaerdere S, De Groote L, Thadani V, Claeys P, Gossiaux F, Van Roost D, Boon P. Generator replacement in epilepsy patients treated with vagus nerve stimulation. Seizure 2005; 14: 89-99. [III]
15) DeGiorgio C, Heck C, Bunch S, Britton J, Green P, Lancman M, Murphy J, Olejniczak P, Shih J, Arrambide S, Soss J. Vagus nerve stimulation for epilepsy: randomized comparison of three stimulation paradigms. Neurology 2005; 65: 317-9. [II]
16) Bunch S, DeGiorgio CM, Krahl S, Britton J, Green P, Lancman M, Murphy J, Olejniczak P, Shih J, Heck CN. Vagus nerve stimulation for epilepsy: is output current correlated with acute response? Acta Neurol Scand 2007; 116: 217-20. [III]
17) Benbadis SR, Nyhenhuis J, Tatum WOT, Murtagh FR, Gieron M, Vale FL. MRI of the brain is safe in patients implanted with the vagus nerve stimulator. Seizure 2001; 10: 512-5. [III]
18) De Tiege X, Legros B, de Beeck MO, Goldman S, Van Bogaert P. Vagus nerve stimulation. J Neurosurg Pediatr 2008; 2: 375-7; author reply 377.
19) Ross IB, Maleeva T, Sutherling WW. Vagus nerve stimulation. J Neurosurg Pediatr 2008; 2: 375; author reply 375.
20) Vassilyadi M, Strawsburg RH. Delayed onset of vocal cord paralysis after explantation of a vagus nerve stimulator in a child. Childs Nerv Syst 2003; 19: 261-3. [IV]
21) Espinosa J, Aiello MT, Naritoku DK. Revision and removal of stimulating electrodes following long-term therapy with the vagus nerve stimulator. Surg Neurol 1999; 51: 659-64. [IV]

Ann Nucl Med (2012) 26:698–706
DOI 10.1007/s12149-012-0629-9

ORIGINAL ARTICLE

Voxel-based comparison of preoperative FDG-PET between mesial temporal lobe epilepsy patients with and without postoperative seizure-free outcomes

Miwako Takahashi · Tsutomu Soma · Kensuke Kawai · Keitraro Koyama · Kuni Ohtomo · Toshimitsu Momose

Received: 21 May 2012 / Accepted: 24 June 2012 / Published online: 19 July 2012

Abstract
Objective This study aims to elucidate differences in preoperative cerebral glucose metabolism between patients who did and did not become seizure free after unilateral mesial temporal lobe epilepsy (mTLE) surgery. We hypothesized that regional glucose metabolism on preoperative fluorodeoxyglucose positron emission tomography (FDG-PET) in patients with seizure-free outcomes differed from that in patients who were not seizure free after appropriate epilepsy surgery for unilateral mTLE. In this study, we compared preoperative FDG-PET findings between these two patient groups by applying a statistical analysis approach, with a voxel-based Asymmetry index (AI), to improve sensitivity for the detection of hypometabolism.
Methods FDG-PET scans of 28 patients with medically refractory mTLE, of whom 17 achieved a seizure-free outcome (Engel class 1 a–b) during a postoperative follow-up period of at least 2 years, were analyzed retrospectively. Voxel values were adjusted by the AI method as well as the global normalization (GN) method. Two types of statistical analysis were performed. One was a voxel severity analysis with comparison of voxel values at the same coordinate, and the other was extent analysis with comparison of the number of significant voxels in the anatomical areas predefined with Talairach's atlas.
Results In the voxel severity analysis, significant hypometabolism restricted to the ipsilateral temporal tip and hippocampal area was detected in the postoperative seizure-free outcome group as compared to controls. No significant area was detected in the non-seizure-free group as compared to controls (family-wise error corrected, $p < 0.05$). With extent analysis using a low threshold, the extents of hypometabolism in the ipsilateral hippocampal, frontal and thalamic areas were larger in the seizure-free than in the non-seizure-free group ($p = 0.01$, 0.03 and 0.01, respectively.) On the other hand, in the contralateral frontal and thalamic areas, extents of hypometabolism were smaller in the seizure-free than in the non-seizure-free group ($p = 0.01$ and 0.01).
Conclusions We found the preoperative distribution of hypometabolism to differ between the two patient groups. Severe hypometabolism restricted to the unilateral temporal lobe, with ipsilateral dominant hypometabolism including mild decreases, may support the existence of an epileptogenic focus in the unilateral temporal lobe and a favorable seizure outcome after mTLE surgery.

Keywords Asymmetry index · FDG-PET · Mesial temporal lobe epilepsy · Postoperative outcome

M. Takahashi · T. Soma · K. Koyama · K. Ohtomo · T. Momose (✉)
Department of Radiology, Graduate School of Medicine, University of Tokyo, 3-1, Hongo 7-Chome, Bunkyo-ku, Tokyo 113-8655, Japan
e-mail: tmomo-tky@umin.ac.jp

T. Soma
Software Development Group, Product Management and Marketing Department, FUJIFILM RI Pharma Co., Ltd, Tokyo, Japan

K. Kawai
Department of Neurosurgery, Graduate School of Medicine, University of Tokyo, Tokyo, Japan

Introduction

Epilepsy surgery is an important treatment for patients with medically refractory epilepsy. Surgery for temporal lobe

epilepsy (TLE) has become an established treatment [1]. While most patients benefit from this surgery, some suffer persistent seizures or recurrence [2].

Fluorodeoxyglucose positron emission tomography (FDG-PET) allows us to measure regional cerebral glucose metabolism semi-quantitatively and to visualize the distribution of altered glucose metabolism [3–5]. In most patients with TLE, interictal FDG-PET shows hypometabolism in the temporal lobe harboring the epileptogenic focus. While the mechanisms underlying metabolic dysfunction have not been elucidated, it is considered to be closely related to epileptogenicity [6–8]. Therefore, the cerebral metabolism distribution on preoperative FDG-PET may differ between the patients with seizure-free outcomes and those with non-seizure-free outcomes after TLE surgery.

Previous studies with FDG-PET showed the presence of hypometabolism in the unilateral temporal lobe ipsilateral to the surgical site to be predictive of a good seizure outcome, and that widespread hypometabolism beyond the temporal lobe is associated with a poor outcome [9–12]. However, hypometabolism is frequently extensive in TLE patients [13]. It is thus necessary to characterize the involvement of the extra-temporal area as well as that of the temporal lobe. However, there is some difficulty in objective evaluation of metabolic changes in the extra-temporal area, because the changes are frequently mild, though they can be detected visually [14].

In this study, we aimed to elucidate the differences in glucose hypometabolism on preoperative interictal FDG-PET between patients with and without seizure-free outcomes. To investigate differences including mild hypometabolism, we applied a voxel-based Asymmetry index (AI) method, in which each voxel value was calculated as the AI instead of using an adjustment method with the cerebral global mean. The AI of hypometabolism is an important index especially for evaluating unilateral hemispheric disease. Some studies have applied AI for the evaluation of hypometabolism; the AI was calculated using the mean count of the ipsilateral and contralateral region of interest (ROI) [11, 15, 16]. Instead of using the mean of the ROI, we calculated the AI for each voxel. Furthermore, we employed two types of analysis. One was voxel severity analysis, which is a widely used method of comparing voxel values at the same coordinate, and the other was extent analysis, in which we counted the number of voxels exceeding a threshold in the predefined volume of interest (VOI) and compared the number of voxels between the two patient groups. We previously reported the combination of this voxel-based AI method and extent analysis to improve the accuracy of epileptogenic zone localization [17]. Therefore, using this method as well as conventional analysis, we attempted to evaluate cerebral cortical hypometabolism.

Materials and methods

Patients and controls

We identified all patients ($n = 145$) who underwent interictal FDG-PET for epilepsy evaluation between 2003 and 2009. Among these patients, 51 were clinically diagnosed as unilateral mesial temporal lobe epilepsy (mTLE) and received surgical treatment of the unilateral hippocampal area, and we selected 28 of these patients (15 males and 13 females, mean age 34.5 $\pm$ 9.7 years) for this study based on the following inclusion criteria: (1) followed up for at least 2 years after surgery; (2) preoperative evaluations including interictal electroencephalography (EEG), interictal and ictal scalp/sphenoidal video-EEG recording, magnetic resonance imaging (MRI), interictal cerebral perfusion single photo emission computed tomography (SPECT), iomazenil SPECT, and interictal FDG-PET had been performed; (3) no space occupying lesion exceeding 1 cm in diameter on MRI; (4) no history of either previous cranial surgery or encephalomyelitis. These preoperative examinations were performed as part of routine evaluations for patients who were surgical candidates for medically refractory epilepsy. Preoperative identification of the epileptogenic zone (EZ) was based on these preoperative evaluations and clinical semiology. FDG-PET was used only for the diagnosis for unilateral mTLE based on decreased FDG in the temporal lobe. Intracranial electrode evaluation was also performed when the concordance of these preoperative evaluations was insufficient.

All patients in this study underwent surgical resection and/or transection of the unilateral hippocampal area [18]. The surgical area was extended to structures neighboring the hippocampus, as necessary. The extent of surgery was decided according to intra-surgical electrocorticography (ECoG) findings.

Patient characteristics are listed in Table 1. Postoperative seizure outcome was evaluated according to the Engel's classification [19] by reviewing medical records. In all analyses, patients were divided into two groups: (1) seizure-free (Engel class 1a and 1b) and (2) non-seizure-free (Engel class 1c and 1d, 2–4). Surgical outcomes were evaluated at 2 years after surgery, but in cases with recurrence within the 2-year follow-up period, outcomes were evaluated at the time of the recurrence. With visual evaluation for clinical diagnosis of mTLE, preoperative FDG-PET showed obvious decrease in the ipsilateral temporal lobe in 20 patients, in other 8 patients, decreases were unobvious or bilateral. There were no significant differences between the seizure-free and non-seizure-free groups in clinical factors, age at onset, epilepsy duration, age at surgery, seizure frequency, surgical side or temporal lobe decreases on preoperative FDG-PET by visual

Table 1 Patient characteristics

	SZ-free ($n = 17$)	Non SZ-free ($n = 11$)	p value
Gender			N.S.
Male	9	6	
Female	8	5	
Age at onset (year)	12.3 ± 10.6	12.0 ± 6.5	N.S.
Duration of epilepsy (year)	23.0 ± 11.8	22.3 ± 9.4	N.S.
Age at surgery (year)	35.3 ± 10.5	32.9 ± 8.5	N.S.
Seizure frequency (number of patients)			N.S.
Daily	6	2	
Weekly	6	2	
Monthly	4	7	
Side of surgery			N.S.
Right	2	5	
Left	15	6	
Visual evaluation of preoperative FDG-PET[a]			N.S.
Ipsi TL decrease	13	7	
Not diagnostic	4	4	

SZ-free seizure-free group, *N.S.* not significant

[a] With visual evaluation for clinical diagnosis of mTLE, "Ipsi TL decrease" means obvious decrease in the ipsilateral temporal lobe on preoperative FDG-PET, and "Not diagnostic" means that the decreases were unobvious or found in the bilateral temporal lobes

evaluation (Fisher's exact test at a significance level of 5 %). Of the 28 patients in this study, 11 were classified into the non-seizure-free group, but most patients had benefitted from surgical therapy. Two patients required a second surgery within the 2-year follow-up period.

FDG-PET scans of the controls were obtained employing an identical protocol for 20 normal controls, as in our previous study [17]. The controls were 11 males and 9 females. Their mean age was 47, range 24–60 years. None had neurological or mental diseases, or any history of cranial surgery or anti-psychotic drug use.

This retrospective study was performed according to the guidelines of the Ethics Review Board of Tokyo University Hospital. Written informed consent was obtained from all patients and controls. We also obtained permission to analyze the clinical data.

FDG-PET acquisition

The patients fasted for at least 5 h and then underwent FDG-PET scanning. A 296 MBq (8 mCi) dose of FDG was injected intravenously, and 45 min later, emission scans were obtained in two-dimensional mode for 10 min, and transmission scans were subsequently obtained to correct for photon attenuation using a $^{68}Ga/^{68}Ge$ rotating rod source. The PET scanner was an Advance NXi (General Electric Medical Systems), with 12096 bismuth-germinate crystals arranged in 18 rings and a 15.2 cm axial field-of-view. The scanner has an intrinsic spatial resolution in the center of the field-of-view of 4.8 mm full width of half maximum (FWHM) and an axial resolution of 4.0 mm FWHM.

During the examination, in a quiet room, the patient rested in the supine position with an eye mask to minimize the confounding factor of environmental noises, and was observed for exclusion of clinical seizure activity. During the scan, the patient's head was kept in the head holder, and when the head moved, a radiology technician corrected the movement according to a mark on the patient's head and a laser pointer device. The FDG-PET data were reconstructed with ordered subset expectation maximization iterative reconstruction, with 2 iterations and 28 subsets. An 8-mm FWHM Gaussian filter was applied to the image. The data were collected for 37 transaxial slices of a 128 × 128 matrix, with a pixel size of 2.03 × 2.03 mm, and 35 successive slices were separated by 4.25 mm.

^{18}F was synthesized using the Cypris Model 370 Cyclotron (Sumitomo Heavy Industries), and FDG was generated with an automated FDG synthesis system (F100: Sumitomo Heavy Industries) on the day of each scan. Radiochemical purity was greater than 95 %.

FDG-PET image processing and statistical analysis

Data analysis was performed using SPM8 and MATLAB version R2011a (MathWorks Inc., Natick, MA, USA). The data analysis steps were: (1) spatial normalization; (2) smoothing; (3) right–left flipping of the images of patients with left TLE; (4) voxel-value adjustment with GN and AI; (5) z score mapping for extent analysis; (6) statistical comparison with voxel severity analysis and (7) extent analysis. This study included patients with right mTLE and patients with left mTLE. The surgical side was set as the right side of the hemisphere, and is described as "ipsilateral" throughout this study.

Processes from (1) to (5) were described in detail in our previous study [17]. In brief, (1) all FDG-PET images (28 mTLE patients and 20 controls) were spatially normalized and (2) smoothed. (3) The images of left mTLE patients were flipped so as to place the affected temporal lobe on the right side in all patients. (4) Voxel values were adjusted by two methods. One was dividing voxel values by the mean value of the whole brain [20]. The other was calculating AI for each voxel. AI images were calculated with non-flipped and flipped images of normalized control and patient images using:

$$V_{AI} = (V_{nf} - V_f)/(V_{nf} + V_f), \quad (1)$$

where V_{AI} represents the AI image, V_{nf} is the non-flipped image, and V_f is the flipped image. AI images were

smoothed using a three-dimensional isotropic Gaussian kernel with a FWHM of 4 mm. (5) For extent analysis, the resulting images were mapped using z scores, calculated on a voxel-by-voxel basis using:

$$Z = (V_m - V_p)/SD, \quad (2)$$

where Z represents the z score, V_m the mean of the corresponding control voxel values, V_p the patient's corresponding voxel values, and SD the standard deviation of the corresponding control voxel values. (6) Voxel severity analysis; to compare the severity of the voxel values of each group (voxel severity analysis), voxel-by-voxel comparison at the same coordinate was performed between the seizure-free group and controls, the non-seizure-free group and controls, and the seizure-free and non-seizure-free groups. Statistical comparisons were performed by t test with SPM. We investigated hypometabolic areas at a height threshold of $p < 0.05$ with family-wise error (FWE) correction for multiple comparisons and an extent threshold of 100 voxels. If no significant voxels were detected, the height threshold was relaxed to $p < 0.001$ (uncorrected). (7) extent analysis; symmetrical right- and left-VOIs were defined by overlapping areas of the right- and left-sided VOIs of the Talairach Deamon Atlas (level 3) [21, 22]. The Talairach Deamon Atlas (level 3) originally showed 55 VOIs on each side. These VOIs were grouped into 7 anatomic areas, including the frontal area, hippocampal area, lateral temporal area, parietal area, occipital area, basal ganglia, and thalamic area on each side, and were converted into the MNI space. Then, we calculated the percentage of the number of voxels exceeding a threshold set at z equal to 0.5, 1.0, 1.5 or 2.0, in these anatomical areas. To compare the extent of hypometabolism of each VOI between the seizure-free and non-seizure-free groups, the Mann–Whitney test was performed. The level of statistical significance was set at a two-sided p value <0.05. The flow chart of data analysis of voxel severity analysis (6) and extent analysis (7) is depicted in Fig. 1.

Statistical analyses except for the voxel severity analysis were performed using SPSS for Windows (version 16; SPSS Inc, Chicago, IL, USA).

Results

Voxel severity analysis

In comparison with controls, the seizure-free group showed a significant decrease in the ipsilateral temporal pole with the GN method ($p < 0.05$, FWE corrected) (Fig. 2), and in the ipsilateral mesial temporal area and temporal pole with the AI method ($p < 0.05$, FWE corrected) (Fig. 3). The voxel peak in these significant areas is listed with the Talairach coordinate, T value, cluster size and anatomical region on Talairach's atlas in Table 2. In the non-seizure-free group as compared with the controls, no significant decrease was detected with the stringent threshold

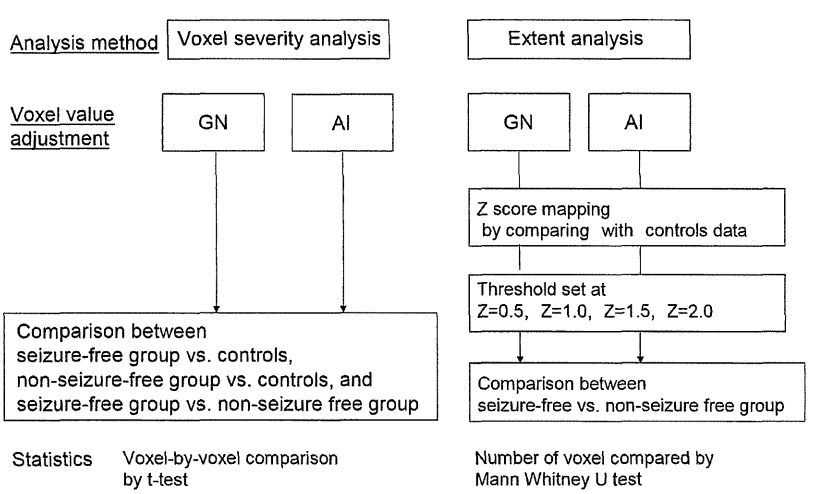

Fig. 1 The flow chart of data analysis depicts two types of statistical analysis; voxel severity and extent analyses. With regards to the voxel-value adjustment, the GN method and the AI method were applied. In the voxel severity analysis, comparison between the seizure-free group and controls, the non-seizure-free group and controls, and the seizure-free and non-seizure-free groups were performed with adjustment for each voxel-value. In the extent analysis, the voxel value was converted to the z score based on control data. Extent was calculated by counting the number of voxels exceeding the predefined threshold. We tried 4 thresholds with z scores ranging from 0.5 to 2.0. Then, the extents of anatomical areas were compared between the seizure-free and non-seizure-free groups

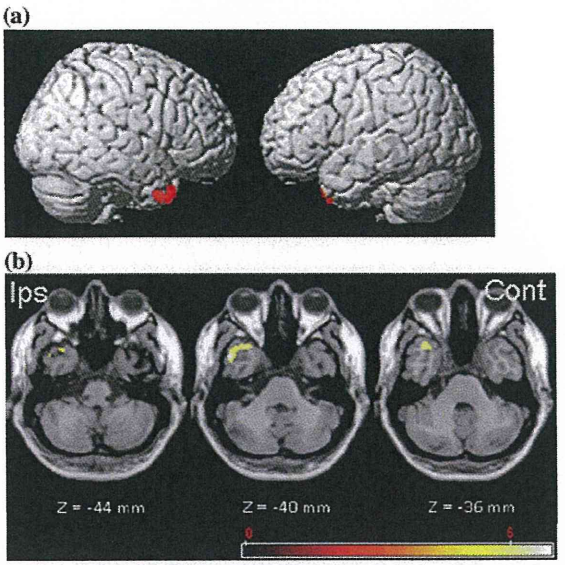

Fig. 2 Comparison between seizure-free group and controls by the GN method ($p < 0.05$ FWE corrected, voxel size >100). **a** Surface view, **b** axial images of areas with significant decreases. *Colored bar* represents t value. *Ips* ipsilateral to the surgical side, *Cont* contralateral to the surgical side. The region in *color* represents the significantly decreased area in the seizure-free group as compared to the controls. The surgical side was set as the right side in this display

($p < 0.05$, FWE corrected) (Figure not shown). With the lenient threshold ($p < 0.001$, uncorrected), a part of the contralateral frontal gyrus, ipsilateral insular area and ipsilateral temporal lobe was detected with AI, but not with GN (Table 3).

Comparison between the seizure-free and non-seizure-free groups revealed no significant voxels detectable with the stringent threshold ($p < 0.05$, FWE corrected). Significant voxels detected with the lenient threshold ($p < 0.001$, uncorrected) are listed in Table 4. The seizure-free group showed a significant decrease in the posterior part of the ipsilateral lentiform nucleus with both the GN and the AI method. On the other hand, when the non-seizure-free group was compared with the seizure-free group, no significantly decreased voxels were detected with the GN method. With the AI method, a significant decrease was detected in the contralateral lentiform nucleus, which is the only contralateral coordinate showing a significant decrease in the seizure-free group as compared to the non-seizure-free group, because the absolute value of AI is equal on the left and right sides at the same coordinate.

Extent analysis

With the AI method and the voxel threshold at $z = 1$, a significant difference was detected in regions of the ipsilateral hippocampal ($p = 0.01$), ipsilateral frontal ($p = 0.03$), ipsilateral thalamic ($p = 0.01$), contralateral frontal ($p = 0.01$) and contralateral thalamic ($p = 0.01$) areas between the seizure-free and non-seizure-free groups. In these areas of the ipsilateral hemisphere, the extent of hypometabolism was larger in the seizure-free than in the non-seizure-free group. On the other hand, in the contralateral frontal area and the thalamus, the extent was smaller in the seizure-free than in the non-seizure-free group. With the AI method and the voxel threshold at $z = 0.5$, a significant difference was detected in the same areas. With the other combinations of the z threshold and the voxel value adjustment method, a significant difference was detected in parts of these areas. With a threshold of $z = 2.0$, only the ipsilateral thalamus showed a significant difference using the GN method ($p = 0.03$) and the AI method ($p = 0.02$). Significantly different areas, median extents and the p values determined with the z threshold using the GN method are listed in Table 5, and those obtained using the AI method in Table 6.

Discussion

We detected differences in the distribution of preoperative cerebral hypometabolism between patients who obtained seizure-free outcomes and those who were not seizure free after surgery. The differences were detected in the bilateral frontal lobe, thalamus, lentiform nucleus and ipsilateral temporal lobe. Our results suggest ipsilateral dominance of hypometabolism in the frontal lobe and subcortical areas, and severe hypometabolism restricted to the ipsilateral temporal lobe to be associated with seizure-free outcomes after unilateral TLE surgery.

In comparison with the controls, the severe hypometabolism detected by voxel severity analysis with the stringent threshold was restricted to the temporal lobe on the surgical side in the group of patients with seizure-free outcomes, which agrees with previous reports [9–12]. In contrast, no significant decreases were detected in the non-seizure-free group. This suggests that the hypometabolism of patients in the non-seizure-free group was less restricted to the unilateral temporal lobe and did not show common features among patients. When using the AI method with the lenient threshold in voxel severity analysis, decreased areas were detected in some areas of the ipsilateral temporal lobe, the ipsilateral insular area, and the contralateral frontal lobe in the non-seizure-free group. These decreases in the ipsilateral temporal lobe and the insular area are considered to be closely related to TLE, because all patients in this study benefitted from surgical therapy involving the unilateral temporal lobe and neighboring structures.

With regard to the extra-temporal lobe area, extent analysis with the AI method was most sensitive for

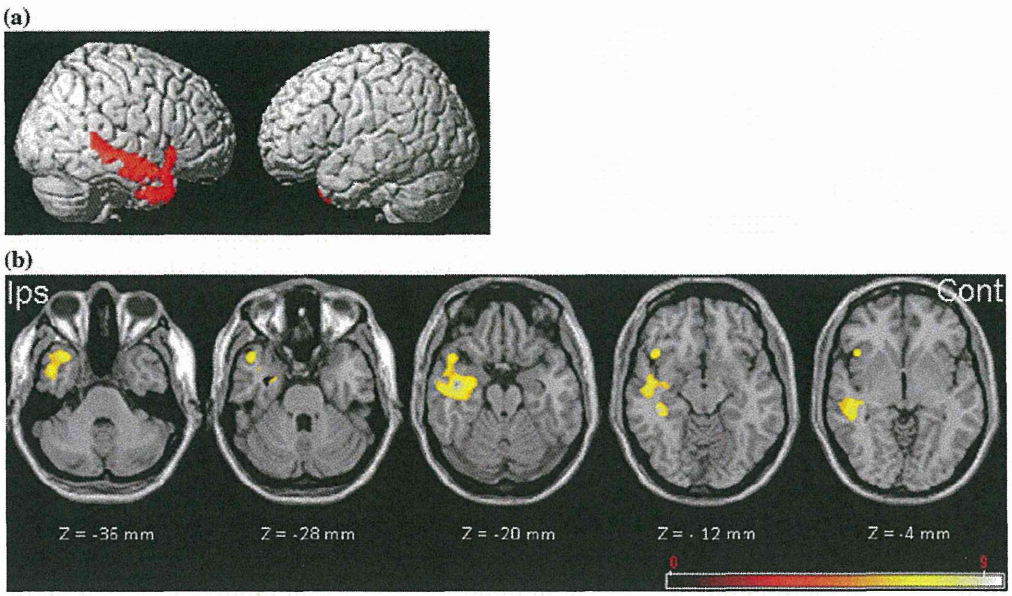

Fig. 3 Comparison between seizure-free group and controls with the AI method ($p < 0.05$ FWE corrected, voxel size > 100). **a** Surface view, **b** axial images of areas with significant decreases. *Colored bar* represents t value. *Ips* ipsilateral to the surgical side, *Cont* contralateral to the surgical side. The region in *color* represents the significantly decreased area in the seizure-free group as compared to the controls. The surgical side was set as the right side in this display

Table 2 Voxel peak in significant area detected by severity voxel analysis in the comparison between the seizure-free group and controls ($p < 0.05$, FWE corrected)

	Coordinates			*T* value	Cluster size	Cerebral regions on Talairach atlas
	X	*Y*	*Z*			
GN method	44	9	−30	6.88	128	Ipsilateral superior temporal gyrus
AI method	45	−37	1	9.43	2039	Ipsilateral superior temporal gyrus

Table 3 Voxel peak in significant area detected by the severity voxel analysis in the comparison between the non-seizure-free group and controls ($p < 0.001$, uncorrected)

	Coordinates			*T* value	Cluster size	Cerebral regions on Talairach atlas
	X	*Y*	*Z*			
GN method	N.S.					
AI method	−42	40	25	6.48	172	Contralateral middle frontal gyrus
	35	13	−34	5.06	136	Ipsilateral superior temporal gyrus
	42	17	−1	5.03	133	Ipsilateral insula
	52	−42	8	4.87	517	Ipsilateral middle temporal gyrus

N.S. not significant

detecting differences between the two patient groups. We consider voxel-based AI to facilitate detection of mild hypometabolism because AI is a sensitive index, especially for hemispheric disease. Furthermore, AI calculation using the voxel-by-voxel approach probably overcomes the disadvantages of VOI-based AI, such as the VOI-dependent fluctuation of AI values and the underestimation caused by the "averaging effect" [23]. The combination with extent analysis allows us to compare the number of voxels exceeding a threshold, even if the threshold is low, corresponding to mild hypometabolism. Also, this method is probably similar to visual evaluation. We usually conduct

Table 4 Voxel peak in significant area detected by the severity voxel analysis in the comparison between the seizure-free and non-seizure-free groups ($p < 0.001$, uncorrected)

Comparison pair and Method	Coordinates			*T* value	Cluster size	Cerebral regions on Talairach atlas
	X	*Y*	*Z*			
SZ-free < Non-SZ-free						
GN method	32	−21	5	4.99	138	Ipsilateral lentiform nucleus
AI method	29	−17	8	5.08	177	Ipsilateral lentiform nucleus
Non SZ-free < SZ-free						
GN method	N.S.					
AI method	−29	−17	8	5.08	177	Contralateral lentiform nucleus[a]

SZ-free seizure-free group

[a] Symmetrical region detected by comparison between seizure-free and non-seizure-free groups performed with AI, because the absolute voxel value is symmetrical

Table 5 Anatomical areas showing significant difference between seizure-free group and non-seizure-free group in analysis with the combination of the GN method and the extent analysis

Threshold	Anatomical area	Median extent (%)[a]		*p* value
		Seizure-free group	Non-seizure-free group	
$z = 0.5$	Ipsilateral hippocampal area	61.5	37.1	0.01
$z = 1.0$	Ipsilateral hippocampal area	44.6	23.7	0.04
$z = 1.5$	Ipsilateral hippocampal area	29.7	14.1	0.04
	Ipsilateral thalamic area	32.5	9.9	0.02
$z = 2.0$	Ipsilateral thalamic area	22.4	3.7	0.03

[a] Median extent (%); Extent (%) is the percentage of the number of voxels exceeding *z* threshold set at $z = 0.5$, 1.0, 1.5, or 2.0, respectively, in the anatomical areas. Median extent (%) is a median value of the extent (%) in each group

Table 6 Anatomical areas showing significant difference between seizure-free group and non-seizure-free group in analysis with the combination of the AI method and the extent analysis

Threshold	Anatomical area	Median extent (%)[a]		*p* value
		Seizure-free group	Non-seizure-free group	
$z = 0.5$	Ipsilateral hippocampal area	70.3	46.5	0.01
	Ipsilateral frontal area	52.6	37.7	0.02
	Ipsilateral thalamic area	58.0	26.9	0.02
	Contralateral frontal area	17.6	28.6	0.03
	Contralateral thalamic area	15.8	37.8	<0.01
$z = 1.0$	Ipsilateral hippocampal area	58.0	30.3	0.01
	Ipsilateral frontal area	36.5	22.7	0.03
	Ipsilateral thalamic area	46.7	14.6	0.01
	Contralateral frontal area	8.5	16.3	0.01
	Contralateral thalamic area	7.4	20.1	0.01
$z = 1.5$	Ipsilateral hippocampal area	45.3	19.3	0.02
	Ipsilateral thalamic area	37.3	7.2	0.01
	Contralateral frontal area	3.9	8.5	0.03
	Contralateral thalamic area	3.3	9.1	0.01
$z = 2.0$	Ipsilateral thalamic area	30.0	3.4	0.02

[a] Median extent (%); Extent (%) is the percentage of the number of voxels exceeding *z* threshold set at $z = 0.5$, 1.0, 1.5, or 2.0 respectively in the anatomical areas. Median extent (%) is a median value of the extent (%) in each group

visual evaluation primarily in consideration of interhemispheric asymmetry and the extent of the asymmetry of each region.

When we used the AI method in extent analysis with a low threshold of $z = 0.5$ or 1.0, the differences were detected in the bilateral frontal lobe and thalamus. With a high threshold of $z = 2.0$, a significant difference was detected only in the ipsilateral thalamus. This may imply that the extent of hypometabolism including mild changes differs between the frontal lobe and the thalamus, and that the extent of relatively severe hypometabolism differs only in the thalamus between the two patient groups. In these areas, contralateral dominance of hypometabolism was observed in the non-seizure-free group, which is consistent with a previous report describing reverse thalamic metabolic asymmetry in patients with poor outcomes [15].

Ipsilateral dominant hypometabolism in the thalamus is frequently observed in patients with TLE [13, 24]. Other studies using ictal perfusion SPECT also showed significant hyperperfusion in the ipsilateral putamen and thalamus as well as the temporal lobe [25]. The degree of thalamic hypometabolism in TLE was associated with a longer duration of epilepsy and a history of secondary generalized convulsions [26]. An animal study also demonstrated persistent hypometabolism in the hippocampus and thalamus in the chronic phase [27]. Based on animal studies, Gale [28] suggested that the thalamus has a reciprocal connection with all limbic structures, which contain a population of neurons vulnerable to irritative activity and also the first to evoke epileptic seizures by stimulation of various forebrain sites. It seems likely that the thalamus is involved in the pathway of transmission of seizure activity. Thalamic hypometabolism may correlate with metabolic dysfunction of the limbic system through dense connections and it may also reflect diffuse hypometabolism of cerebral cortices collectively.

Ipsilateral frontal hypometabolism reportedly has a close relationship with TLE. Comparing ictal perfusion SPECT with interictal FDG-PET, concordance of abnormalities of ictal hyperperfusion and hypometabolism was detected predominantly on the ipsilateral orbitofrontal and insular cortex [29]. In addition, the ipsilateral orbitofrontal area showed hyperperfusion during the initial phase of the seizure, shifting to hypoperfusion in a later phase, suggesting the propagation of epileptic activity followed by surround inhibition [25]. In this study, we also demonstrated a correlation between the extent of hypometabolism in the ipsilateral frontal lobe and those of the ipsilateral hippocampal area in seizure-free outcome patients ($R = 0.52$, $p = 0.02$, Spearman rank correlation test). In contrast, this correlation was not detected in non-seizure-free outcome patients. Therefore, ipsilateral frontal hypometabolism may support the existence of an EZ in the ipsilateral temporal area. However, the interpretation of frontal hypometabolism requires caution, because depression and cognitive impairment, which are frequently associated with TLE, also show frontal hypometabolism [30–32]. The consistency of the laterality of predominant hypometabolism between the temporal and frontal lobes may facilitate distinguishing whether hypometabolism is closely related to TLE itself or a secondary cognitive dysfunction due to epilepsy.

All patients in this study were preoperatively diagnosed as having mTLE based on comprehensive examinations and semiology. Electrical abnormalities with intra-surgical ECoG were detected in the hippocampal area of the surgical side, and the extent of surgery for the temporal area and surrounding structures was decided based on the ECoG findings. If the EZ exists far from the surgical field, which cannot be investigated by ECoG, then, surgical intervention cannot be performed, and seizure control may therefore be less likely to be obtained. Our non-seizure-free patients showed contralateral dominant hypometabolism in the frontal lobe and thalamus, which suggests that the metabolic dysfunction related to epileptogenesis may not be limited to the area around the ipsilateral temporal lobe.

We have to mention about the limitation of image analysis applying asymmetry index. Asymmetry index cannot differentiate between the ipsilateral hypometabolism and the contralateral hypermetabolism. Van Bogaert et al. reported that the contralateral temporal hypermetabolism was detected in patients with unilateral mTLE with voxel-based statistical analysis. They interpreted it as reflecting compensatory mechanisms, but also gave a caution of the possibility of subclinical epileptic activity [33]. In this study, we visually evaluated the preoperative FDG-PET images for diagnosis of mTLE, and did not detect any focal increased area with suspected epileptic discharge. In addition, GN method as well as AI method was applied, and there was no contradictive results between the two methods, but we cannot exclude the possibility of the slight contralateral hypermetabolism contributing to improve the sensitivity of AI method.

The results of this study confounded neither the surgical method and nor the surgical area. The hypometabolism in the temporal lobe was used only for the diagnosis of mTLE. In the future study, multiple regression analysis should be performed to assess the influences of our observations and other factors including MRI results, intra-surgical ECoG findings and surgical method in a large number of patients.

In conclusion, differences in the distribution of preoperative hypometabolism between patients with and without seizure-free outcomes were detected with voxel-based statistical analysis. Differences were detected in the frontal lobe and the subcortical area as well as the temporal lobe. The ipsilateral predominant hypometabolism including mild changes in the

frontal lobe and thalamus may support epileptogenesis being limited to the ipsilateral temporal lobe and surrounding area. Not only whether hypometabolism is restricted to the temporal lobe, but also the laterality of hypometabolism in the frontal lobe and the thalamus may facilitate predicting seizure outcomes after unilateral TLE surgery.

Acknowledgments We would like to thank the staff of our Nuclear Medicine Department and our secretaries, for their contributions to this study.

References

1. Wiebe S, Blume WT, Girvin JP, Eliasziw M. A randomized, controlled trial of surgery for temporal-lobe epilepsy. N Engl J Med. 2001;345:311–8.
2. Salanova V, Markand O, Worth R. Longitudinal follow-up in 145 patients with medically refractory temporal lobe epilepsy treated surgically between 1984 and 1995. Epilepsia. 1999;40:1417–23.
3. Sokoloff L, Reivich M, Kennedy C, Des Rosiers MH, Patlak CS, Pettigrew KD, et al. The [14C]deoxyglucose method for the measurement of local cerebral glucose utilization: theory, procedure, and normal values in the conscious and anesthetized albino rat. J Neurochem. 1977;28:897–916.
4. Reivich M, Kuhl D, Wolf A, Greenberg J, Phelps M, Ido T, et al. The [18F]fluorodeoxyglucose method for the measurement of local cerebral glucose utilization in man. Circ Res. 1979;44:127–37.
5. Alavi A, Dann R, Chawluk J, Alavi J, Kushner M, Reivich M. Positron emission tomography imaging of regional cerebral glucose metabolism. Semin Nucl Med. 1986;16:2–34.
6. Henry TR, Babb TL, Engel J Jr, Mazziotta JC, Phelps ME, Crandall PH. Hippocampal neuronal loss and regional hypometabolism in temporal lobe epilepsy. Ann Neurol. 1994;36:925–7.
7. Vinton AB, Carne R, Hicks RJ, Desmond PM, Kilpatrick C, Kaye AH, et al. The extent of resection of FDG-PET hypometabolism relates to outcome of temporal lobectomy. Brain. 2007;130:548–60.
8. Matheja P, Kuwert T, Ludemann P, Weckesser M, Kellinghaus C, Schuierer G, et al. Temporal hypometabolism at the onset of cryptogenic temporal lobe epilepsy. Eur J Nucl Med. 2001;28:625–32.
9. Radtke RA, Hanson MW, Hoffman JM, Crain BJ, Walczak TS, Lewis DV, et al. Temporal lobe hypometabolism on PET: predictor of seizure control after temporal lobectomy. Neurology. 1993;43:1088–92.
10. Manno EM, Sperling MR, Ding X, Jaggi J, Alavi A, O'Connor MJ, et al. Predictors of outcome after anterior temporal lobectomy: positron emission tomography. Neurology. 1994;44:2331–6.
11. Theodore WH, Sato S, Kufta CV, Gaillard WD, Kelley K. FDG-positron emission tomography and invasive EEG: seizure focus detection and surgical outcome. Epilepsia. 1997;38:81–6.
12. Choi JY, Kim SJ, Hong SB, Seo DW, Hong SC, Kim BT, et al. Extratemporal hypometabolism on FDG PET in temporal lobe epilepsy as a predictor of seizure outcome after temporal lobectomy. Eur J Nucl Med Mol Imaging. 2003;30:581–7.
13. Henry TR, Mazziotta JC, Engel J Jr. Interictal metabolic anatomy of mesial temporal lobe epilepsy. Arch Neurol. 1993;50:582–9.
14. Hashiguchi K, Morioka T, Yoshida F, Kawamura T, Miyagi Y, Kuwabara Y, et al. Thalamic hypometabolism on 18FDG-positron emission tomography in medial temporal lobe epilepsy. Neurol Res. 2007;29:215–22.
15. Newberg AB, Alavi A, Berlin J, Mozley PD, O'Connor M, Sperling M. Ipsilateral and contralateral thalamic hypometabolism as a predictor of outcome after temporal lobectomy for seizures. J Nucl Med. 2000;41:1964–8.
16. Lee SK, Lee DS, Yeo JS, Lee JS, Kim YK, Jang MJ, et al. FDG-PET images quantified by probabilistic atlas of brain and surgical prognosis of temporal lobe epilepsy. Epilepsia. 2002;43:1032–8.
17. Soma T, Momose T, Takahashi M, Koyama K, Kawai K, Murase K, et al. Usefulness of extent analysis for statistical parametric mapping with asymmetry index using inter-ictal FGD-PET in mesial temporal lobe epilepsy. Ann Nucl Med. 2012;26:319–26.
18. Shimizu H, Kawai K, Sunaga S, Sugano H, Yamada T. Hippocampal transection for treatment of left temporal lobe epilepsy with preservation of verbal memory. J Clin Neurosci. 2006;13:322–8.
19. Engel J Jr, Van Ness PC, Rasmussen TB, Ojemann LM. Outcome with respect to epileptic seizures. In: Engel Jr J, editor. Surgical treatment of the epilepsies. New York: Raven Press; 1993. p. 609–21.
20. Fox PT, Mintun MA, Reiman EM, Raichle ME. Enhanced detection of focal brain responses using intersubject averaging and change-distribution analysis of subtracted PET images. J Cereb Blood Flow Metab. 1988;8:642–53.
21. Lancaster JL, Rainey LH, Summerlin JL, Freitas CS, Fox PT, Evans AC, et al. Automated labeling of the human brain: a preliminary report on the development and evaluation of a forward-transform method. Hum Brain Mapp. 1997;5:238–42.
22. Lancaster JL, Woldorff MG, Parsons LM, Liotti M, Freitas CS, Rainey L, et al. Automated Talairach atlas labels for functional brain mapping. Hum Brain Mapp. 2000;10:120–31.
23. Rubin E, Dhawan V, Moeller JR, Takikawa S, Labar DR, Schaul N, et al. Cerebral metabolic topography in unilateral temporal lobe epilepsy. Neurology. 1995;45:2212–23.
24. Khan N, Leenders KL, Hajek M, Maguire P, Missimer J, Wieser HG. Thalamic glucose metabolism in temporal lobe epilepsy measured with 18F-FDG positron emission tomography (PET). Epilepsy Res. 1997;28:233–43.
25. Dupont P, Zaknun JJ, Maes A, Tepmongkol S, Vasquez S, Bal CS, et al. Dynamic perfusion patterns in temporal lobe epilepsy. Eur J Nucl Med Mol Imaging. 2009;36:823–30.
26. Benedek K, Juhasz C, Muzik O, Chugani DC, Chugani HT. Metabolic changes of subcortical structures in intractable focal epilepsy. Epilepsia. 2004;45:1100–5.
27. Guo Y, Gao F, Wang S, Ding Y, Zhang H, Wang J, et al. In vivo mapping of temporospatial changes in glucose utilization in rat brain during epileptogenesis: an 18F-fluorodeoxyglucose-small animal positron emission tomography study. Neuroscience. 2009;162:972–9.
28. Gale K. Subcortical structures and pathways involved in convulsive seizure generation. J Clin Neurophysiol. 1992;9:264–77.
29. Bouilleret V, Boyet S, Marescaux C, Nehlig A. Mapping of the progressive metabolic changes occurring during the development of hippocampal sclerosis in a model of mesial temporal lobe epilepsy. Brain Res. 2000;852:255–62.
30. Lambert MV, Robertson MM. Depression in epilepsy: etiology, phenomenology, and treatment. Epilepsia. 1999;40:S21–47.
31. Hosokawa T, Momose T, Kasai K. Brain glucose metabolism difference between bipolar and unipolar mood disorders in depressed and euthymic states. Prog Neuropsychopharmacol Biol Psychiatry. 2009;33:243–50.
32. Takaya S, Hanakawa T, Hashikawa K, Ikeda A, Sawamoto N, Nagamine T, et al. Prefrontal hypofunction in patients with intractable mesial temporal lobe epilepsy. Neurology. 2006;67:1674–6.
33. Van Bogaert P, Massager N, Tugendhaft P, Wikler D, Damhaut P, Levivier M, et al. Statistical parametric mapping of regional glucose metabolism in mesial temporal lobe epilepsy. Neuroimage. 2000;12:129–38.